Associations between fetal heart rate variability and umbilical cord occlusions-induced neural injury: An experimental study in a fetal sheep model.

Louise Ghesquière, Romain Perbet, Laure Lacan, Yasmine Ould Hamoud, Morgane Stichelbout, Dyuti Sharma, Sylvie Nguyen The Tich, Laurent Storme, Veronique Debarge, Julien de Jonckheere, et al.

HAL Id: hal-04536346

https://hal.univ-lille.fr/hal-04536346

Submitted on 8 Apr 2024

ORIGINAL RESEARCH ARTICLE

Associations between fetal heart rate variability and umbilical cord occlusions-induced neural injury: An experimental study in a fetal sheep model

Louise Ghesquière[1,2] | Romain Perbet[3] | Laure Lacan[1,4] | Yasmine Hamoud[1,2] | Morgane Stichelbout[3] | Dyuti Sharma[1,5] | Sylvie Nguyen[1,4] | Laurent Storme[1,6] | Véronique Houfflin-Debarge[1,2] | Julien De Jonckheere[1,7] | Charles Garabedian[1,2]

[1]Evaluation of Health Technologies and Medical Practices (METRICS) – ULR 2694, University of Lille, Centre Hospitalier Universitaire de Lille, Lille, France

[2]Department of Obstetrics, Centre Hospitalier Universitaire de Lille, Lille, France

[3]Department of Anatomopathology, Centre Hospitalier Universitaire de Lille, Lille, France

[4]Department of Neuropediatrics, Centre Hospitalier Universitaire de Lille, Lille, France

[5]Department of Pediatric Surgery, Centre Hospitalier Universitaire de Lille, Lille, France

[6]Department of Neonatology, Centre Hospitalier Universitaire de Lille, Lille, France

[7]Clinical Investigation Center – Technological Innovation (CIC-IT 1403), Centre Hospitalier Universitaire de Lille, Lille, France

Correspondence
Louise Ghesquière, CHU Lille, Department of Obstetrics, Avenue Eugène Avinée, 59037 Lille Cedex, France.
Email: louise.ghesquiere@chru-lille.fr

Abstract

Introduction: This study evaluated the association between fetal heart rate variability (HRV) and the occurrence of hypoxic–ischemic encephalopathy in a fetal sheep model.

Material and methods: The experimental protocol created a hypoxic condition with repeated cord occlusions in three phases (A, B, C) to achieve acidosis to pH <7.00. Hemodynamic, gasometric and HRV parameters were analyzed during the protocol, and the fetal brain, brainstem and spinal cord were assessed histopathologically 48 h later. Associations between the various parameters and neural injury were compared between phases A, B and C using Spearman's rho test.

Results: Acute anoxic–ischemic brain lesions in all regions was present in 7/9 fetuses, and specific neural injury was observed in 3/9 fetuses. The number of brainstem lesions correlated significantly and inversely with the HRV fetal stress index ($r = -0.784$; $p = 0.021$) in phase C and with HRV long-term variability ($r = -0.677$; $p = 0.045$) and short-term variability ($r = -0.837$; $p = 0.005$) in phase B. The number of neurological lesions did not correlate significantly with other markers of HRV.

Conclusions: Neural injury caused by severe hypoxia was associated with HRV changes; in particular, brainstem damage was associated with changes in fetal-specific HRV markers.

KEYWORDS
autonomic nervous system, fetal heart rate, heart rate variability, intrapartum hypoxic–ischemia, neural injury, umbilical cord compression

---

---

1 | INTRODUCTION

In developed countries, 30% of neonatal encephalopathy cases are associated with evidence of intrapartum hypoxic-ischemic encephalopathy (HIE).[1] Despite concerted efforts to improve the identification of intrapartum fetal hypoxia, no standard clinical technique is currently in use, and techniques such as cardiotocography analysis, computerized fetal heart rate (FHR) analysis, ST analysis and fetal blood sampling are inadequate for predicting HIE.[2,3] Graham et al. found that abnormalities during the last hour of FHR monitoring before delivery were poor predictors of neonatal HIE, with an area under the receiver-operating characteristic curve of 0.68 for total decelerations.[4] A large, unmasked, randomized controlled trial (the INFANT trial) reported no significant developmental differences at the 2-year assessment between the use of computerized FHR interpretation during labor and visual analysis.[5] Similarly, Ruth et al. showed that fetal acid-base status did not correlate with the risk of HIE and poor perinatal brain damage prediction by umbilical cord arterial pH.[6] More recent studies have confirmed that pH is a poor predictor of the long-term outcome after perinatal asphyxia.[6–8]

The intrapartum assessment of fetal hypoxic ischemia remains an important challenge in perinatal medicine, in which the aim is to screen for at-risk neonates and to prevent HIE during labor. One current approach is the analysis of the autonomic nervous system activity, which plays a major role in fetal homeostasis and which influences the FHR. Heart rate is regulated continuously by the action of the sympathetic and parasympathetic nervous systems on the sinoatrial node. Fetal heart rate variability (HRV) assesses the variations in time interval between two heartbeats (RR interval) and reflects autonomic nervous system activity. Several HRV indices are based on either time or spectral analysis of the RR intervals identified with fetal electrocardiography (ECG).[9] Time-domain analysis includes indices such as the standard deviation of the normal-to-normal RR interval (SDNN), the root mean square of successive differences between adjacent RR intervals (RMSSD), or short-term and long-term variability (STV and LTV, respectively); the latter was developed specifically for fetal HRV analysis.[10] Frequency (or spectral) HRV analysis can distinguish several frequency domains: very low frequencies reflecting thermoregulation and endocrine activity, low frequencies (LFs) reflecting sympathetic and parasympathetic activities associated with the baroreflex, and high frequencies (HFs) specifically linked to parasympathetic activity.[11,12]

Our team developed the fetal stress index (FSI) based on an original HRV analysis method[11] that combined time and spectral analysis.[10] In previous experimental studies using a model of repeated cord occlusion in fetal sheep, we demonstrated that this index was related to variations in parasympathetic activity[11] and correlated with acid-base status.[13] Such a biomarker may constitute a new pathway for evaluating fetal well-being during labor.[14]

HRV is also a promising tool for predicting early neural injury. An association between abnormal HRV and brain impairment has been reported in the perinatal period, although the data remain incomplete.[15] Direct subcortical or brainstem injury leading to autonomic dysfunction is one possible pathophysiological mechanism,[16] and data from animal models support this hypothesis.[17] Considering this association, HRV has been also suggested as a possible marker of neural injury in HIE following perinatal asphyxia.[18]

The main objective of our study was to evaluate the associations between HRV biomarkers and the occurrence of HIE in a fetal sheep model. The secondary objective was to evaluate the associations between hemodynamic and gasometric biomarkers and the occurrence of HIE.

Key message

Fetal heart rate variability markers correlated with brainstem injury induced by an experimental umbilical cord occlusion model in fetal sheep.

2 | MATERIAL AND METHODS

2.1 | Surgical preparation

Near-term pregnant sheep (breed "Ile de France" INRA) with a gestational age of 124 ± 1 days (term = 145 days) underwent our previously described surgical procedure.[13,19,20] Ewes were anesthetized by a vascular infusion of 500 ml of Ringer's lactate, followed by premedication with 0.3 ml intravenous Sedaxylan (xylazine 20 mg/ml, Dechra). The ewes were induced with 5% isoflurane before intubation, and anesthesia was maintained with 2% isoflurane. A midline abdominal incision was made to expose the uterus, and the fetus was partially exteriorized for instrumentation. Two catheters (4 Fr diameter, Arrow) were placed in the fetal axillary arteries, one on each side. The first was used for continuous arterial blood pressure measurement and the other for arterial blood sampling. Four ECG electrodes (Mywire 10, Maquet) were placed on the fetal intercostal muscles to record fetal ECG. An additional catheter was placed within the amniotic sac to measure pressure within the amniotic space. An inflatable silicone occluder (OC16; In Vivo Metric) was placed around the umbilical cord, and the volume of saline solution required to achieve complete occlusion was recorded. If a ewe had multiple fetuses, only one was instrumented and included in the experiment. The twin that was easier to access during surgery was chosen to avoid twisting the uterus.

2.2 | Experimental protocol

Ewes were acclimatized to the experiment room for 1 h daily in the presence of the primary investigators. The experimental protocol began 4 days after the surgery. Fetal arterial catheters and the intra-amniotic catheter were connected to pressure sensors (Pressure

Monitoring Kit) connected to a multiparametric monitor (Monitor Merlin, Hewlett Packard). Arterial blood pressure was measured from the blood pressure phasic signal and referenced to the intra-amniotic pressure. ECG electrodes were connected to the multiparametric monitor. Hemodynamic data were recorded continuously throughout the experiment.

After a 1-h baseline period, repetitive umbilical cord occlusions (UCOs) were performed by injecting an isotonic solution into the occluder to obtain a total occlusion for 1 min (Figure S1). The protocol was divided into three 1-h periods, as described by Prout et al.[21] UCOs were repeated every 5 min during the first phase (phase A), every 3 min during the second phase (phase B) and every 2 min during the third phase (phase C). During the baseline period and at the end of each UCO phase, the HRV markers and gasometric parameters were recorded during a 5-min period with no UCO. The protocol was stopped if the pH reached ≤6.90 to avoid fetal death during the protocol.

Euthanasia was administered at the end of the experimental procedure, 2 days after or, in cases of *in utero* fetal death or death, during surgery. Euthanasia was performed by intravenous injection of 6 ml/50 kg of T61 (1 ml containing embutramide 200 mg + mebezonium 26.92 mg + tetracaine 4.39 mg, MSD). The fetal brain, brainstem and spinal cord were extracted and fixed immediately in 4% neutrally buffered formalin.

Blood samples were taken from the arterial catheter 1 min after the end of the last UCO of each phase (A, B and C). Gasometric parameters were then measured using an iSTAT1 blood analyzer (iSTAT1 System, Abbott Point of Care Inc.) using CG4+ cartridges. FHR, mean arterial blood pressure (MAP) and mean intra-amniotic pressure were read from the multiparametric scope at the same time. MAP was corrected by subtracting the intra-amniotic pressure as follows: corrected MAP = observed MAP – observed mean intra-amniotic pressure. We also recorded the MAP and FHR nadir during the last occlusion of each phase.

2.3 | HRV markers

Our team has reported on the autonomic response to fetal acidosis through HRV analysis in a fetal sheep model.[13,19,20] In those studies, we focused on the most common HRV indexes as well as on two markers used for fetal monitoring in clinical practice.[20] We also developed a specific algorithm to analyze the fetal parasympathetic activity.[19] To use similar methodology, we used the same indexes in this study. The details of ECG signal processing and HRV indexes computation are described below.

ECG analysis for fetal RR series computation was conducted offline using an automatic R-wave detection algorithm.[22] RR series artifacts were detected automatically and replaced by linear interpolation using a specific RR series filtering algorithm.[23] This patented filtering algorithm is already implemented in HRV analysis medical devices used in neonates (NIPE Monitor, MDoloris Medical Systems) and during surgery (ANI Monitor, MDoloris Medical Systems), and its ability to detect and replace any erroneous samples

with high accuracy has been established. RMSSD and SDNN were computed over 540 RR intervals (ie ~3 min, considering a basal FHR of 180 bpm). RMSSD is related to parasympathetic nervous system activity, whereas SDNN evaluates autonomic nervous system global activity.[10]

We also investigated the STV and LTV. STV was computed for 1 min after a 4-Hz resampling of the RR series and was defined as the mean absolute difference between successive 3.75 s of averaged RR interval epochs >1 min (ie 16 epochs). LTV represents the difference between the maximum and minimum of the 16 epochs. The RR series was isolated in a 64-s moving window and resampled at 8 Hz. Spectral HRV analyses were performed using a four-coefficient Daubechies wavelet transform. We then computed the LF component, which corresponds to the spectral power from 0.04 to 0.15 Hz. We also computed the HF component, which corresponds to the spectral power >0.15 Hz.

We developed a specific HRV marker. FSI, which reflects relative parasympathetic activity, has been described previously.[20,24] The RR series was isolated in a 64-s moving window and was resampled at 8 Hz. The mean value (M) was computed as follows:

$$M = \frac{1}{N} \sum_{i=1}^{N} RR_i,$$

where RR_i represents the RR sample values and N represents the number of samples in the window. M is then subtracted from each sample of the window as: $RR'_i = (RR_i - M)$. The norm value (S) was then calculated as follows:

$$S = \sqrt{\sum_{i=1}^{N} \left(RR'_i\right)^2},$$

and each RR'_i was divided by S to yield $RR''_i = RR'_i / S$. The normalized RR'' series was then high-pass filtered at >0.15 Hz using a four-coefficient Daubechies wavelet-based filter to keep only HF oscillations.

The magnitude of these oscillations was then computed as the area between the local maximum envelope and the local minimum envelope (Figure S2). To increase the time sensitivity, the envelope was divided in four 16-s subareas, A1, A2, A3 and A4. AUC_{min} was computed as the minimum value of A1, A2, A3 and A4, and FSI was defined as FSI = 100 × (5.1 × AUC_{min} + 1.2)/12.8 to obtain a value between 0 and 100.

STV, LTV, HF, LF and FSI were computed every second and averaged over a 176-s period to eliminate the inter-window variability. HRV markers were evaluated at the end of each 5-min stable period (ie with no UCO) between phases A, B and C. Before performing the HRV analysis, RR series quality was checked visually for these three periods to verify the absence of remaining artifacts and that <25% of the original RR series was modified by the RR series artifact-filtering algorithm. For RR series that failed the visual check, we used the continuous invasive arterial blood pressure signal for RR series construction and HRV analysis. If an artifact remained, the record was excluded from the analysis.

To avoid including outlying FHR values resulting from the last UCO, the beginning of these stable periods was not analyzed for HRV parameter estimation. Within these stable periods, SDNN and RMSSD were computed between $t = 2$ min and $t = 5$ min. STV, LTV, HF, LF and FSI were computed for 4 min (64 s + 176 s) between $t = 60$ s and $t = 5$ min.

2.4 | Tissue analysis

Entire fetal brain and spinal cord were extracted and fixed immediately in 4% neutrally buffered formalin. After 1 month in 4% buffered formalin, the cerebrum was separated from the brainstem and the cerebellum. Each part was cut into slices of 3–4 mm, and each slice was embedded in paraffin, sectioned at 5 μm, and stained with hematoxylin–eosin–saffron. All slides were screened and the maximum count of ischemic neurons on a field (0.30 mm^2) was retained in each area of interest: cortex (frontal, parietal, temporal, occipital, entorhinal), basal ganglia, hippocampus, brainstem and cerebellum (cerebellar cortex and dentate nucleus). Ischemic neurons were defined by shrinkage, eosinophilic or vacuolated cytoplasm, and peripherally located hyperchromatic nuclei (Figure S3).[25–29] Two pathologists counted the lesions independently. In cases of disagreement, the slides were then reviewed collaboratively. The ischemic neuron counts in each region were summed for a global acute anoxic–ischemic lesion score. The pathologists were blind to the hypoxic status of the fetuses.

2.5 | Statistical analyses

Given the small sample size, only nonparametric statistical tests were used. Numerical data are described as median (first and third quartiles). Differences between occlusion phases A, B and C were evaluated using a Friedman nonparametric test for repeated measurements, followed by a Wilcoxon test when deemed significant. Associations between biomarkers (hemodynamics, HRV and gasometrics) and neurological lesions were assessed using marker values after phases A, B and C to evaluate (i) the ability of markers to distinguish fetuses with or without neurological lesions and (ii) correlations between markers and the number of neurological lesions using Spearman's rho test. To consider the variability between fetuses, we also investigated the correlations between the number of neurological lesions and marker evolution between phases A and B and between phases B and C.

Each biomarker was compared in terms of the total neural injury and the lesions in each brain region (basal ganglia, brainstem, cerebellum, cortex and hippocampus). A p-value <0.05 was considered to be significant for the Spearmen rho test. For the Bonferroni correction for multiple comparisons, a p-value <0.025 was considered to be significant for comparison between phases A, B and C. Statistical analyses were performed using IBM SPSS Statistics (version 20.0; IBM Corp.).

2.6 | Ethical approval

The anesthesia, surgical, and experimental protocols were consistent with recommendations by the Ministry of Higher Education, Research and Innovation, and the study was approved by the Animal Experimentation Ethics Committee, France (CEEA #2016121312148878). This manuscript is compliant with the ARRIVE guidelines for reporting animal research.[30] All methods were performed in accordance with relevant guidelines and regulations.

3 | RESULTS

Fourteen pregnant sheep underwent the surgical procedure. Two fetuses died during the first 2 days after surgery. Twelve fetuses underwent the experimental procedure. Two experimental procedures were stopped because of rupture of the occlusion balloon in one and per protocol fetal death in the other. One fetus was later excluded because of severe chronic neural injury that occurred before the protocol (laminar necrosis, slit-like cavities in the deep cortical area, gliosis, and macrophage infiltration). Finally, nine experimental fetuses were analyzed, and HRV analysis was performed using the ECG data for eight of these fetuses. Only one fetus required analysis of the invasive blood pressure signal.

3.1 | Histological analysis

The two pathologists agreed about the analysis for 7/9 fetuses, and only required collaborative reassessment. Acute anoxic–ischemic neural injury was found in 7/9 fetuses. The brain regions with the greatest number of lesions were, in descending order, the cerebral cortex (115 lesions), basal ganglia (39 lesions), cerebellum (34 lesions), hippocampus (20 lesions) and brainstem (18 lesions) (Table S1). In the hippocampus, all lesions were observed in the Ammon horn. The average number of acute anoxic–ischemic neural injuries per fetus was 25.1, with a minimum of 0 (two fetuses) and a maximum of 83. Basal ganglia lesions were observed in 6/9 fetuses. Brainstem lesions were observed in 3/9 fetuses.

3.2 | Gasometric parameters and neural injury

The pH decreased progressively from 7.28 (first to third quarter: 7.23–7.35) after phase A to 7.10 (7.07–7.27) after phase B, and 6.98 (6.84–7.08) after phase C ($p = 0.001$) (Table 1). Three of nine fetuses reached a pH <6.90. By contrast, lactate concentration increased progressively from 6.0 mmol/L (3.4–8.3) after phase A to 12.8 mmol/L (7.3–15.3) after phase B, and 15.9 mmol/L (13.6–16.3) after phase C ($p < 0.001$). The partial pressure of oxygen (PO$_2$) did not differ between the three phases and values were ~16 mmHg during each phase, indicating that fetal oxygenation returned to the preocclusion level after the occluder release. The partial pressure of carbon dioxide (PCO$_2$) increased progressively from A to B to C: 50.6 mmHg (48.5–56.2), 54.0 mmHg

TABLE 1 Comparison of hemodynamics, gasometrics and heart rate variability parameters in the different occlusion phases (A, B and C) (Friedman + Wilcoxon test)

| | Occlusion phase | | | |
	A (n = 9)	B (n = 9)	C (n = 8)	p^a
HR (bpm)	178 (151–187)	189 (158–202)	175 (150–192)	0.687
MAP (mmHg)	58 (47–65)	62 (51–66)	64 (54–68)	0.239
HRocc (bpm)	90 (91–96)	82 (68–96)	79 (54–92)	0.368
MAPocc (mmHg)	56 (51–62)	54 (43–62)	37 (20–50)[b,c]	**0.004**
pH	7.28 (7.23–7.35)	7.10 (7.07–7.27)[b]	6.98 (6.84–7.08)[b,c]	**0.001**
PO_2 (mmHg)	16.0 (11.5–17.0)	15.0 (13.0–17.5)	16.5 (13.5–18.8)	0.639
PCO_2 (mmHg)	50.6 (48.5–56.2)	54.0 (52.5–63.1)[b]	64.9 (55.1–87.0)[b,c]	**0.002**
BD (mmol / L)	−3.0 (−4.5 to 1.5)	−11.0 (−15.0 to −2.5)[b]	−16.0 (−19.8 to −14)[b,c]	**<0.001**
Lactate (mmol / L)	6.0 (3.4–8.3)	12.8 (7.3–15.3)[b]	15.9 (13.55–16.3)[b,c]	**<0.001**
FSI	54.9 (46.8–70.5)	55 (47.3–67.8)	75.8 (66–80.2)[b,c]	**0.01**
STV(ms)	3.34 (2.97–5.42)	4.55 (3.98–5.20)	4.35 (2.61–7.46)	0.197
LTV(ms)	35.3 (29.3–44.2)	48.9 (41.8–68.4)	45.8 (25.3–64.3)	0.197
SDNN	19.4 (16.0–20.6)	19.3 (15.2–22.1)	19 (17.3–24.1)	0.607
RMSSD	13.1 (6.4–21.8)	12.8 (12.1–16.9)	19.9 (16.4–24.6)	0.417
LF	0.14 (0.04–0.22)	0.13 (0.07–0.21)	0.20 (0.12–0.53)	0.687
HF	0.06 (0.02–0.13)	0.06 (0.04–0.12)	0.12 (0.08–0.27)	0.417

Note: Data are presented as median (1st–3rd quartile). Bold value indicates $p < 0.025$.

Abbreviations: BD, base deficit; FSI, Fetal Stress Index; HF, high frequency; HR, heart rate; LF, low frequencies; LTV, long-term variability; MAP, mean arterial pressure; RMSSD, root mean square of successive differences; SDNN, standard deviation of the normal-to-normal RR interval; STV, short-term variability.

Statistical analysis: [a]Friedman test; Wilcoxon test; [b]$P < 0.025$ vs A; [c]$P < 0.025$ vs B.

(52.5–63.1) and 64.9 mmHg (55.1–87.0), respectively ($p = 0.002$), indicating a respiratory component of the maximal fetal acidosis. Base excess and lactate concentration increased significantly in phases A, B and C ($p < 0.001$), indicating a predominant metabolic component to the increasing acidosis across the phases.

PCO_2 correlated significantly with lesions in the cerebral cortex and hippocampus in phase A (0.800, $p = 0.010$ and 0.685, $p = 0.042$, respectively) and in phase B (0.741, $p = 0.022$ and 0.712, $p = 0.032$). Lactate concentration correlated inversely with lesions in the cerebellum in phase B (−0.756; $p = 0.019$). None of the gasometric parameters correlated significantly with the number or type of total neural injury, basal ganglia lesions or brainstem lesions in any phase (Table 2). Comparisons between phases A and B and between phases B and C confirmed the lack of correlation between the number of cerebral lesions and pH, base deficit, and lactate concentration. By contrast, changes in PCO_2 and PO_2 correlated significantly (Table S2).

3.3 | Hemodynamic parameters and neural injury

FHR did not differ significantly between the three phases: 178, 189 and 175 bpm for phases A, B and C, respectively ($p = 0.687$). MAP also did not differ between the three phases: 58, 62 and 64 mmHg, respectively ($p = 0.239$) (Table 1). FHR decelerations during occlusions seemed to become progressively more severe during each series (Figure 1). MAP during occlusions decreased progressively by 19 mmHg (34%) from phase A to C (56 mmHg to 37 mmHg, $p = 0.004$), indicating mild to severe hypotension in phase C (Table 1).

Correlations between neural injury and hemodynamic parameters are described in Table 3. FHR during occlusions in phase B correlated significantly with the total neural injury (0.812, $p = 0.008$) and the number of cortex lesions (0.724; $p = 0.028$) (Table 3). MAP during occlusions correlated significantly with brainstem lesions in phase A (−0.871; $p = 0.005$), cerebral cortex and hippocampus lesions in phase B (−0.782, $p = 0.022$ and −0.777, $p = 0.023$, respectively), and total neural injury and cerebral cortex lesions in phase C (−0.893, $p = 0.007$ and −0.927, $p = 0.003$, respectively). Correlations between MAP during occlusion in phase C and basal ganglia and hippocampus lesions were not significant (−0.703, $p = 0.078$ and −0.730, $p = 0.063$, respectively). The progress from phase A to B and from phase B to C confirmed correlations between the number of lesions and the changes in MAP and MAP and FHR nadir (Table S2).

TABLE 2 Correlation between gasometric parameters and the number of acute anoxic-ischemic neurological lesions, basal ganglia lesions, brainstem lesions, cerebellum lesions, cortex lesions and hippocampus lesions

	Phase	Total neurological lesions[a]	Basal ganglia lesions	Brainstem lesions	Cerebellum lesions	Cortex lesions	Hippocampus lesions
pH	A	0.134; 0.731	0.094; 0.811	0.279; 0.467	0.598; 0.089	−0.162; 0.678	−0.009; 0.982
	B	0.332; 0.383	0.282; 0.462	0.520; 0.151	0.588; 0.096	−0.038; 0.922	0.079; 0.839
	C	−0.479; 0.420	−0.195; 0.643	−0.371; 0.365	−0.12; 0.977	−0.479; 0.230	−0.038; 0.922
PCO_2 (mmHg)	A	0.594; 0.092	0.477; 0.194	−0.04; 0.919	−0.222; 0.565	**0.800; 0.010**	**0.685; 0.042**
	B	0.485; 0.185	0.383; 0.309	−0.04; 0.919	−0.504; 0.166	**0.741; 0.022**	**0.712; 0.032**
	C	0.647; 0.083	0.366; 0.373	0.509; 0.198	0.206; 0.624	0.577; 0.134	0.524; 0.183
$PO2$ (mmHg)	A	−0.158; 0.684	−0.043; 0.912	0.148; 0.705	0.546; 0.128	−0.413; 0.269	−0.440; 0.236
	B	−0.105; 0.787	0.000; 1.000	−0.02; 0.959	0.405; 0.279	−0.343; 0.366	−0.350; 0.356
	C	0.078; 0.854	0.221; 0.599	0.242; 0.564	0.372; 0.364	0.049; 0.908	0.186; 0.659
BD (mmol/L)	A	0.265; 0.491	0.231; 0.550	0.06; 0.878	0.477; 0.195	0.038; 0.922	0.168; 0.666
	B	0.308; 0.420	0.240; 0.533	0.467; 0.205	0.573; 0.107	−0.060; 0.878	0.053; 0.892
	C	−0.339; 0.411	−0.111; 0.793	−0.306; 0.461	0.319; 0.441	−0.441; 0.274	−0.349; 0.397
Lactate (mmol/L)	A	−0.151; 0.669	−0.128; 0.743	−0.090; 0.819	−0.530; 0.142	0.051; 0.896	−0.088; 0.822
	B	−0.424; 0.255	−0.363; 0.337	−0.52; 0.151	**−0.756; 0.019**	−0.068; 0.861	−0.123; 0.752
	C	−0.012; 0.978	0.049; 0.909	0.082; 0.846	−0.533; 0.173	0.147; 0.728	0.026; 0.952

Note: The correlations between the gasometric markers during phases A, B and C and brain lesions are shown. Results are presented as *r*-values (Spearman's Rho coefficient); *p* was significant if <0.05. Bold value indicates $p < 0.05$.

Abbreviation: BD, base deficit.

[a]Total neurological lesions = lesions of all the different regions (basal ganglia, brainstem, cerebellum, cortex, hippocampus).

3.4 | HRV parameters

Most HRV indices did not differ significantly between the three phases (Table 1). Only FSI changed significantly: from 54.9 (46.8–70.5) in phase A to 75.8 (66–80.2) in phase C ($p < 0.01$), and from 55 (47.3–67.8) in phase B to 75.8 (66–80.2) in phase C ($p < 0.01$). FSI, LTV and STV each correlated negatively with the number of brainstem lesions: for FSI in phase C (−0.784; $p = 0.021$) and for LTV (−0.677; $p = 0.045$) and STV (−0.837; $p = 0.005$) in phase B (Table 3). SDNN in phase C correlated negatively with the number of brainstem lesions (−0.825, $p = 0.012$) and hippocampus lesions (−0.766, $p = 0.027$). Neural injury did not correlate significantly with other HRV indices such as RMSSD, HF and LF.

A scatterplot of the total and brainstem lesion counts as a function of LTV and STV values in phase B is presented in Figure 2; and a scatterplot as a function of FSI and SDNN in phase C is presented in Figure 3. FSI, LTV, STV and SDNN did not distinguish between the two fetuses with no neural injury and those with neural injury. However, the three fetuses with brainstem lesions had a lower STV (<4.3 ms) in phase B (Figure 4), lower FSI (<75) in phase C and lower SDNN (<18 ms) in phase C compared with fetuses with no brainstem lesions (Figures 5 and 6).

Analysis of the progress from phase A to B and from phase B to C showed that none of the HRV markers correlated significantly with the number of lesions (Table S3), which appears to indicate that the absolute values of HRV indexes are more relevant than their differences between two phases.

4 | DISCUSSION

In this animal model of severe fetal acidosis in near-term fetal sheep, neural injuries were obtained, predominantly in the cerebral cortex. The pH did not correlate with the number of lesions identified at the end of the experimental procedure.

The number of brain lesions correlated with variation in hemodynamic parameters, especially with MAP during occlusion, but not with HRV markers. Lesion numbers in the brainstem, cerebral cortex and hippocampus correlated with MAP during occlusion. Brainstem lesion numbers were associated with changes in HRV, especially STV, LTV, SDNN and FSI. It is of note that in fetuses with brainstem damage, the FSI was either unchanged or moderately increased, in contrast to fetuses with no brainstem damage. The FSI reflects the state of the parasympathetic system, which suggests that the parasympathetic system was unable to adapt in fetuses with brainstem lesions. The FSI increased at the onset of acidosis, which confirmed the increased activity of the parasympathetic system in the fetal acidosis condition. Gasometric parameters did not correlate significantly with neural injury, regardless of location.

Predicting HIE during labor is a major issue. HIE is defined as neonatal encephalopathy secondary to systemic hypoxia and reduced cerebral perfusion leading to ischemic injury that may be focal or diffuse. Early identification of infants at risk of complications such as encephalopathy is important for instituting prompt intervention. Fetal acidosis is a risk factor for neurological outcomes such as convulsions and neonatal encephalopathy. Kelly et al. showed a
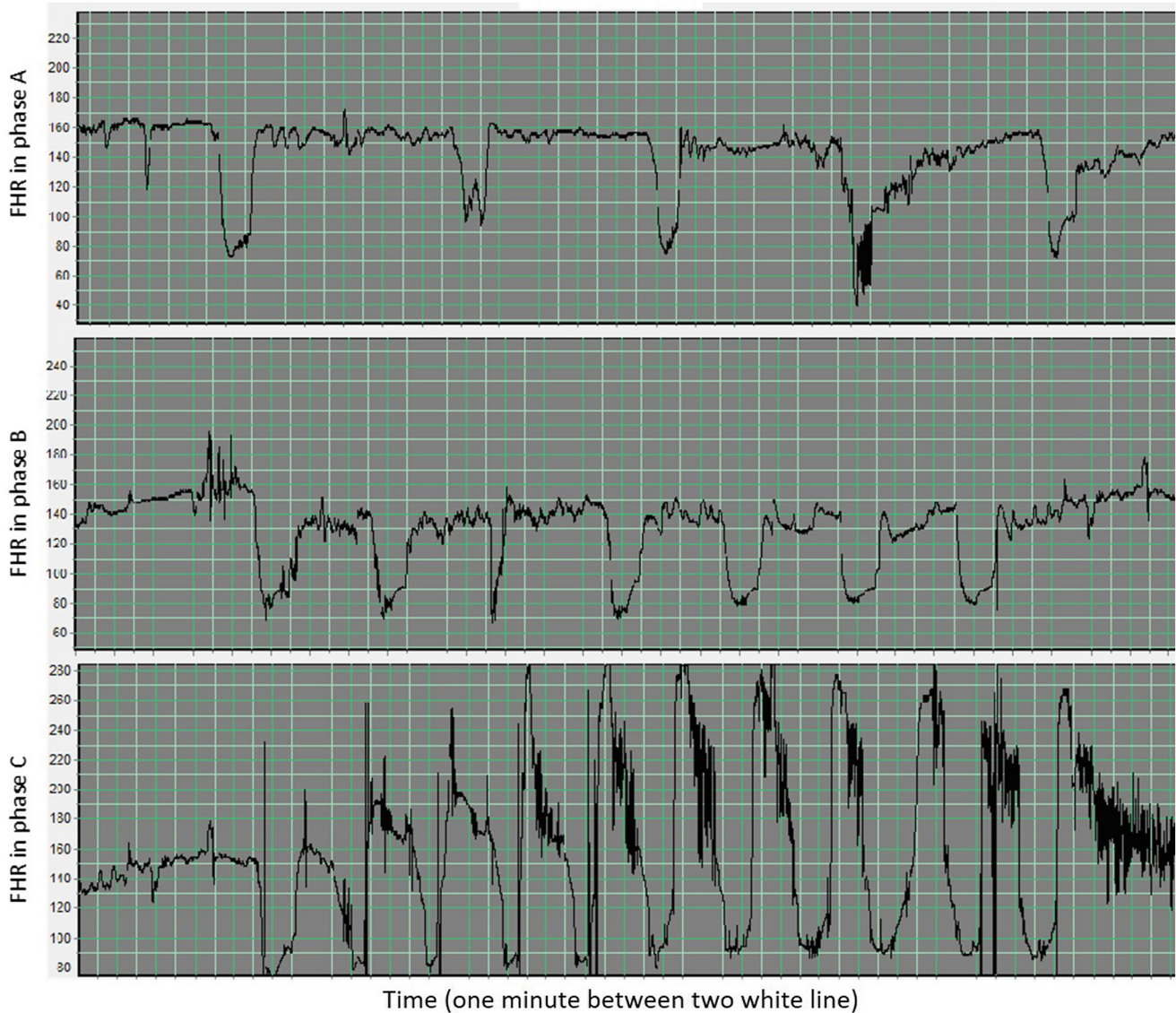
FIGURE 1 Evolution of fetal heart rate decelerations during umbilical cord occlusions in phase (A) phase (B) and phase (C). FHR: fetal heart rate. Umbilical cord occlusions (UCOs) were repeated every 5 minutes during the first phase (phase A), every 3 minutes during the second phase (phase B), and every 2 minutes during the third phase (phase C)

dose-dependent relation between the degree of acidosis within 1 h of delivery and the likelihood of adverse neonatal and later neuro-developmental outcomes.[31] In that study, the combined prevalence rates of death or cerebral palsy were 3%, 10% and 39% at pH nadirs of 6.9–6.99, 6.8–6.89 and <6.8, respectively.

However, a large proportion of newborns with very low pH/high base deficit values are asymptomatic and do not require special neonatal care.[32] This idea is strengthened by studies of long-term developmental outcomes. Hafström et al. studied 234 neonates with umbilical arterial pH <7.05 and base deficit in the extracellular fluid >12.0 mmol/L, who appeared healthy at birth. Outcome measures at age 6.5 years showed no differences in neurological or behavioral problems in these children compared with control children.[33] In a study of 883 infants, Ruth et al. reported that the sensitivity and positive predictive value for adverse outcomes were 21% and 8%

for low pH, 12% and 5% for high lactate concentration, and 12% and 19% for low 5-min Apgar score, respectively.[6] They concluded that metabolic acidosis determined in blood from the umbilical artery at birth is a poor predictor of perinatal brain damage. However, the relation between umbilical cord blood pH or base deficit at birth and the infant's immediate condition and risk for subsequent encepha-lopathy has not been well characterized.[18] In our model, pH did not correlate significantly with neural injury. However, it is difficult to draw firm conclusions about the predictive ability of pH because our model did not allow us to investigate the progression of neural injury between phases A, B and C, and the association between pH and neural injury was compared only using the final number of lesions.

The relation between fetal blood pH and intrapartum neural in-jury is poorly understood. By contrast, via a decrease in fetal sys-temic arterial blood pressure, fetal cardiovascular decompensation

TABLE 3 Correlation between hemodynamics and heart rate variability markers and the number of acute anoxic-ischemic neurological lesions, basal ganglia lesions, brainstem lesions, cerebellum lesions, cortex lesions and hippocampus lesions

	Phase	Total neurological lesions[a]	Basal Ganglia lesions	Brainstem lesions	Cerebrum lesions	Cortex lesions	Hippocampus lesion
HR	A	0.225; 0.561	0.181; 0.641	0.182; 0.640	−0.095; 0.807	0.254; 0.509	0.067; 0.865
	B	0.385; 0.306	0.519; 0.152	−0.139; 0.720	0.180; 0.644	0.451; 0.223	0.167; 0.668
	C	0.012; 0.977	0.147; 0.728	−0.221; 0.598	−0.598; 0.118	0.167; 0.693	0.000; 1.000
MAP	A	−0.613; 0.079	−0.568; 0.110	−0.475; 0.196	**−0.708; 0.033**	−0.338; 0.374	−0.338; 0.374
	B	−0.371; 0.325	−0.614; 0.079	−0.306; 0.423	−0.358; 0.344	−0.240; 0.533	−0.186; 0.632
	C	−0.263; 0.528	−0.464; 0.247	−0.165; 0.696	0.170; 0.688	−0.344; 0.404	−0.332; 0.422
HR occ	A	0.477; 0.194	0.386; 0.304	0.070; 0.857	0.341; 0.370	0.391; 0.299	0.089; 0.821
	B	**0.812; 0.008**	0.621; 0.074	0.448; 0.226	0.496; 0.175	**0.724; 0.028**	0.518; 0.153
	C	−0.479; 0.230	−0.342; 0.408	−0.550; 0.158	0.267; 0.523	−0.479; 0.230	−0.664; 0.073
MAP occ	A	−0.575; 0.136	−0.274; 0.511	**−0.871; 0.005**	−0.427; 0.292	−0.442; 0.272	−0.491; 0.217
	B	−0.635; 0.091	−0.679; 0.064	−0.498; 0.209	0.195; 0.643	**−0.782; 0.022**	**−0.777; 0.023**
	C	**−0.893; 0.007**	−0.703; 0.078	−0.418; 0.350	−0.036; 0.938	**−0.927; 0.003**	−0.730; 0.063
FSI	A	−0.393; 0.295	−0.162; 0.678	0.120; 0.759	0.248; 0.520	−0.553; 0.122	−0.571; 0.108
	B	−0.494; 0.177	−0.443; 0.233	0.139; 0.720	−0.256; 0.505	−0.434; 0.243	−0.369; 0.329
	C	−0.515; 0.192	−0.464; 0.247	**−0.784; 0.021**	0.279; 0.504	−0.577; 0.134	−0.677; 0.065
LTV	A	0.151; 0.699	0.238; 0.537	0.299; 0.435	−0.077; 0.844	0.306; 0.423	0.281; 0.464
	B	−0.075; 0.847	−0.077; 0.845	**−0.677; 0.045**	0.171; 0.660	0.034; 0.931	−0.167; 0.668
	C	−0.108; 0.799	−0.146; 0.729	−0.481; 0.227	0.036; 0.932	−0.123; 0.772	−0.396; 0.332
STV	A	−0.025; 0.949	0.187; 0.629	0.169; 0.663	−0.009; 0.983	0.094; 0.811	0.070; 0.857
	B	−0.402; 0.284	−0.255; 0.507	**−0.837; 0.005**	−0.051; 0.896	−0.255; 0.507	−0.483; 0.188
	C	−0.228; 0.588	−0.244; 0.560	−0.440; 0.275	0.073; 0.864	−0.270; 0.518	−0.511; 0.196
SDNN	A	0.059; 0.881	0.204; 0.598	0.299; 0.435	−0.342; 0.368	0.264; 0.493	0.281; 0.464
	B	0.126; 0.748	−0.077; 0.845	0.040; 0.919	−0.291; 0.448	0.264; 0.493	0.123; 0.753
	C	−0.623; 0.099	−0.683; 0.062	**−0.825; 0.012**	0.121; 0.775	−0.651; 0.081	**−0.766; 0.027**
RMSSD	A	−0.460; 0.213	−0.187; 0.629	−0.020; 0.959	−0.359; 0.343	−0.383; 0.309	−0.369; 0.329
	B	−0.050; 0.898	−0.068; 0.862	0.129; 0.740	−0.103; 0.793	0.034; 0.931	−0.132; 0.735
	C	0.000; 1.000	−0.268; 0.520	−0.481; 0.227	0.206; 0.624	−0.049; 0.908	−0.192; 0.650
LF	A	−0.444; 0.232	−0.221; 0.567	−0.239; 0.536	−0.581; 0.101	−0.196; 0.614	−0.176; 0.651
	B	0.017; 0.966	0.102; 0.794	−0.518; 0.153	−0.034; 0.930	0.187; 0.629	−0.079; 0.840
	C	−0.072; 0.866	−0.049; 0.909	−0.481; 0.227	0.061; 0.887	−0.110; 0.795	−0.370; 0.366
HF	A	−0.460; 0.213	−0.187; 0.629	−0.020; 0.959	−0.359; 0.343	−0.383; 0.309	−0.369; 0.329
	B	−0.033; 0.932	0.128; 0.743	−0.408; 0.275	0.017; 0.965	0.077; 0.845	−0.228; 0.554
	C	0.060; 0.888	−0.073; 0.863	−0.385; 0.346	0.097; 0.819	0.012; 0.977	−0.230; 0.584

Note: Tables 3 show the correlations between hemodynamics and HRV markers during phases A, B and C and brain lesions. Results are presented in *r*-values (Spearman's Rho coefficient); *p* was significant if <0.05. Bold value indicates $p < 0.05$.

Abbreviations: BD, base deficit; FSI, Fetal Stress Index; HF, high frequencies; HR, heart rate; LF, low frequencies; LTV, long-term variability; MAP, mean arterial pressure; RMSSD, root mean square of successive differences; SDNN, standard deviation of the normal-to-normal RR interval; STV, short-term variability.

[a]Total neurological lesions = lesions of all the different regions (basal ganglia, brainstem, cerebellum, cortex, hippocampus).

leads to a precipitous decrease in cerebral perfusion pressure, which results in cerebral ischemia and injury.[18,34] We found an association between hypotension and hypoxia with fetal neural injury. The hypotension observed during occlusion in phase C (−19 mmHg, from 56 mmHg in phase A to 37 mmHg in phase C; *p* = 0.004) correlated with the total number of neurological lesions, especially in the cerebral cortex. We note high *r*-values between hypotension in phase C with basal ganglia and hippocampus lesions.

During hypoxia, an initial increase in blood pressure maintains cerebral blood flow,[34] although, because of ongoing myocardial decompensation, the blood pressure reduces to the normal or subnormal blood pressure and cerebral blood flow (and therefore nutrient
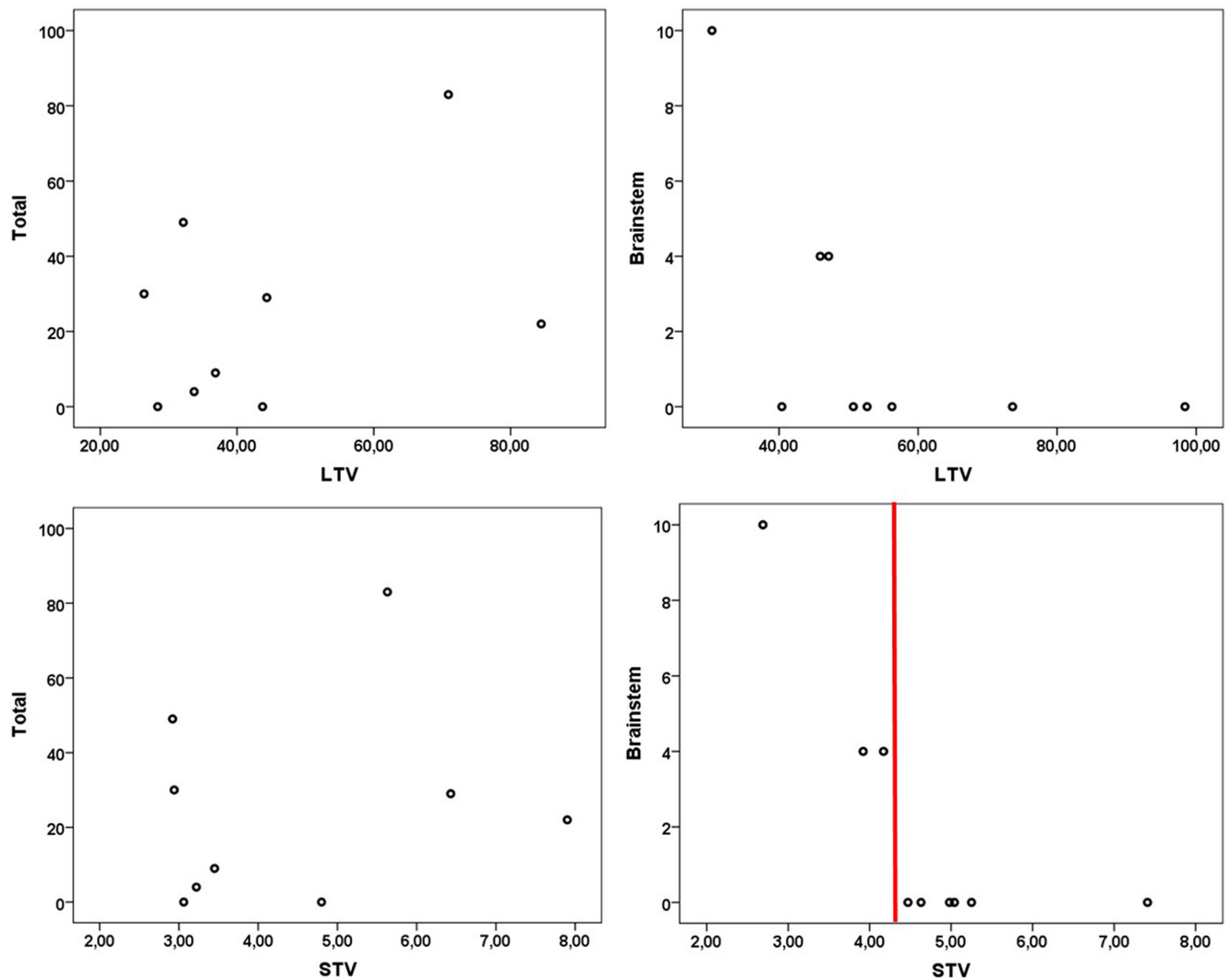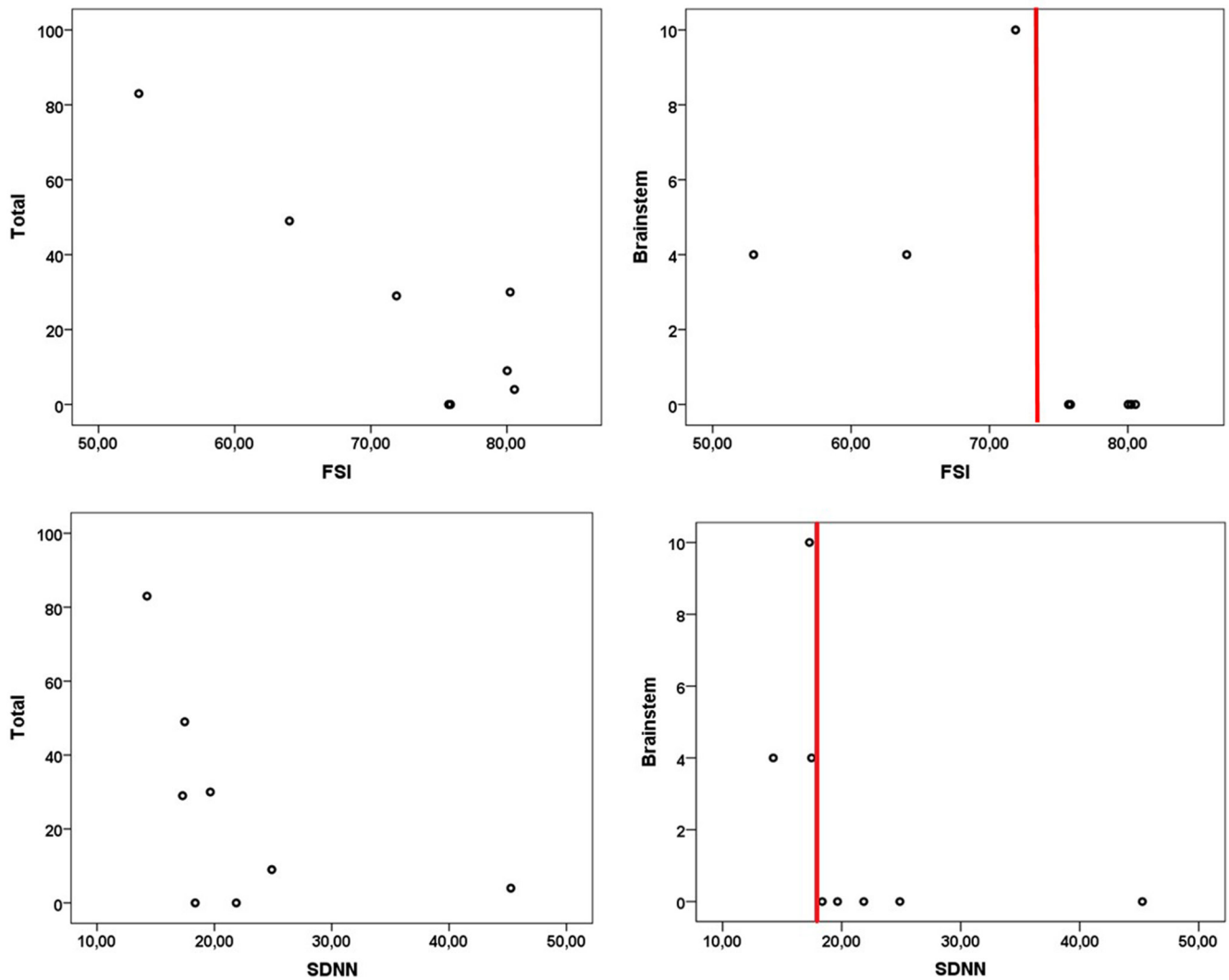
FIGURE 2 Total number of neural and brainstem lesions as a function of short-term variability (STV) and long-term variability (LTV) values per fetal sheep in phase B. One point: one fetal sheep. Vertical axis: number of lesions (total and brainstem). Horizontal axis: LTV and STV values

and oxygen supply) is compromised. Severe hypotension (defined as a decrease by >20 mmHg) has been shown to compromise cerebral perfusion and precipitates hypoxic-ischemic injury in animal models.[34–36] In models of cerebral ischemia in fetal sheep at term, seizure activity was prominent and histological analysis showed lesions in the cerebral cortex, hippocampus and basal ganglia.[37,38] Therefore, it is important to improve the ability to identify fetuses at risk of hypotension that may lead to hypoxic-ischemic injury during labor.[34] Unfortunately, fetal blood pressure cannot be measured during human labor.

Given the poor ability of pH to predict HIE, HRV as a potential biomarker for predicting HIE has been investigated.[18,39] In studies of near-term fetal sheep, Gold et al. reported that an anomaly-detection algorithm applied to the widely used HRV (RMSSD) reliably detected the onset of cardiovascular decompensation. Yamaguchi et al. highlighted the need for novel HRV approaches to capture the complex HRV response to HIE injury or other insults that result in perinatal

brain injury.[40] They elucidated the potential pathophysiological mechanism by which direct subcortical or brainstem injury leads to autonomic dysfunction.[37,41] This condition is supported by our findings of correlations between several HRV markers and brainstem lesions; that is, FSI, SDNN, STV and LTV correlated with the number of brainstem lesions. However, none of these four markers was superior to the others in predicting lesions.

Fetal HRV reflects the complex interaction of sympathetic and parasympathetic activities, which in turn are influenced by fetal baroreceptors and chemoreceptors.[19,38,42] Acute hypoxemia, detected by the carotid body chemoreceptors, stimulates the autonomic brainstem centers to increase both parasympathetic and sympathetic activities, predominantly parasympathetic tone.[13,40] In our study, although all fetal HRV markers tended to increase with acidosis, only the increase in FSI was significant. However, we also found significant inverse correlations between the number of brainstem lesions and STV and LTV in phase B, and FSI and SDNN

FIGURE 3 Total number of neural and brainstem lesions as a function of fetal stress index (FSI) and standard deviation of the normal-to-normal RR interval (SDNN) values per fetal sheep in phase C. One point: one fetal sheep. Vertical axis: number of lesions (total and brainstem). Horizontal axis: FSI and SDNN values
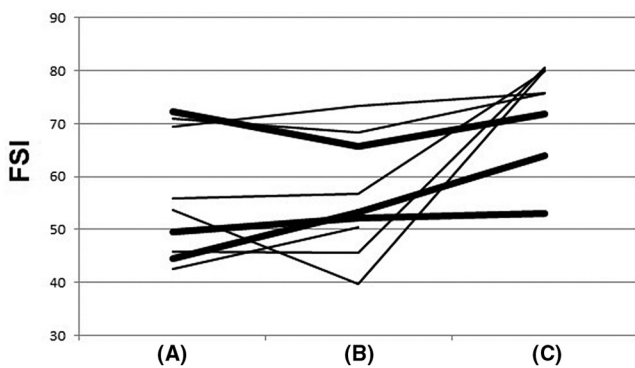
FIGURE 4 Individual tracing of fetal stress index (FSI) evolution against phases (phases A, B and C). Evolution of FSI during phases A, B and C of experimental protocol (horizontal ax). One line = one fetal sheep. Thick lines = fetuses with lesions in the brainstem
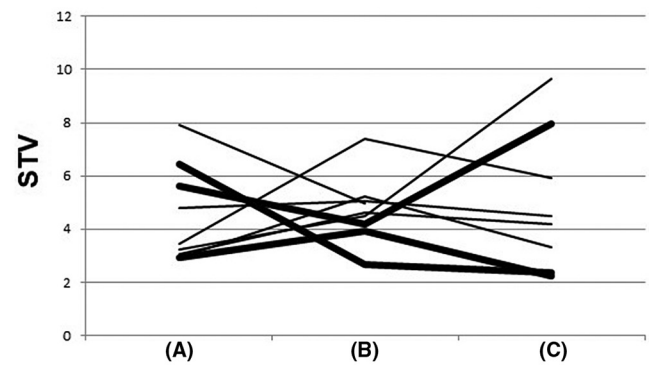
FIGURE 5 Individual tracing of short-term variability (STV) evolution against phases (phases A, B and C). Evolution of STV during phase A, B and C of experimental protocol (horizontal axis). One line = one fetal sheep. Thick lines = fetuses with lesions in the brainstem
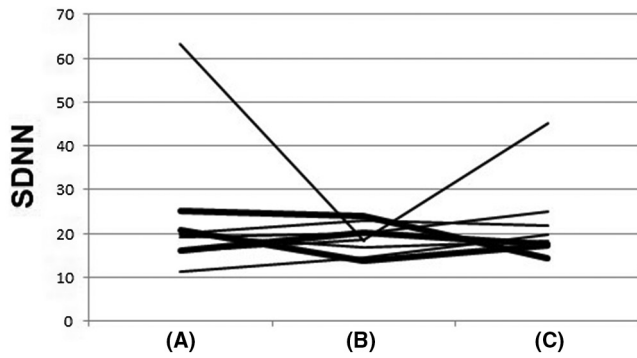
FIGURE 6 Individual tracing of short-term variability evolution against phases (phases A, B and C). Evolution of standard deviation of the normal-to-normal RR interval (SDNN) during phase A, B and C of experimental protocol (horizontal axis). One line = one fetal sheep. Thick lines = fetuses with lesions in the brainstem

in phase C. Brainstem injury can lead to autonomic dysfunction and modifications of fetal HRV. Of note, in fetuses with brainstem damage, both FSI and SDNN were either unchanged or moderately increased, in contrast to fetuses in which there was no brainstem damage. George et al. observed a reduction in fetal HRV indexes (STV, LTV, SDNN, RMSSD) measured in the latent phase during the near- to mid-gestation period; these changes may be related to HIE brain injury, particularly to the autonomic centers of the brainstem.[37] These findings suggest that suppression of fetal HRV after HIE was not related to lesion severity but rather to brainstem lesions. In our study, both FSI and SDNN were higher in phase C in the absence of brainstem lesions. This suggests that increased FSI and SDNN may indicate positive adaptations of the fetus to hypoxia, as evidenced by the absence of neurological damage. The STV and LTV results are more difficult to explain because they correlated significantly in phase B but not in phase C. More experimental studies are needed to explain this puzzling result.

Our primary goal was to study the associations between HRV indices and hypoxia/acidemia. The main strength of this study is that we were able to evaluate the associations between HRV and neural injury. The best way to define the relevant outcomes of intrapartum monitoring studies is an issue that has often been discussed in the literature and during expert panels.[43] There is a lack of clarity or consensus regarding the goals of intrapartum monitoring, especially regarding the role of intrapartum acidemia in the etiology of fetal neural injury.[6,7,16] Neurological outcome, as proposed in the INFANT trial, should be the gold standard.[5]

The only correlations found were between brainstem lesions and HRV. Pathophysiologically, this seems logical because the brainstem participates in the autonomic nervous system, which regulates HRV. However, brainstem lesions are less frequent and are described in the literature as occurring later and as a sign of severe hypoxia.[44] Our histological analysis found many more lesions in the cortex and basal ganglia, which suggests that these areas of the brain are more sensitive to hypoxia. We found no correlation between the number of these lesions and HRV. It is therefore possible that HRV is

sensitive only to severe lesions, but this remains to be confirmed by other studies.

Our study has some limitations. We observed only two fetuses without lesions, which suggests that our findings should be interpreted with caution, while nevertheless encouraging exploration of this promising line of research on HIE prevention. Another limitation is the use of correlational analysis. Our small sample may have led to bias in the interpretation of the results of the correlational analysis. Therefore, the results obtained using this method should be confirmed in a larger population for external validation. Although we used an animal model of human gestation, the reproducibility of our physiological findings and their applications to human fetuses must be established.[45] Fetal hypoxia was obtained through umbilical cord compression, as described in previous studies by other teams.[21,40,46,47] However, this reflects only a part of the mechanism of hypoxia during contractions, which can also be caused by compression of the uteroplacental vessels.[38] Moreover, the histological analysis of the brain was performed after an experimental protocol, and we do not know exactly when the neurological lesions occurred. Continuous EEG recording may have helped address this limitation and is planned for future experiments. In addition, the gestational age we assessed is the nearest possible to full term that can currently be assessed in sheep. Surgery closer to term is difficult because of the high risk of inducing labor before the experiment can be completed.[21,46,47] Finally, a pH <6.90 signaled the end of our experiment. Despite the differences between models using pH as a cutoff to show minimal injury,[21,48] compared with those using hypotension,[46] we observed mild to severe hypotension during phase C.

5 | CONCLUSION

Fetal hypotension and HRV were associated with the presence of neurological lesions. These findings suggest that HRV analysis may be a promising tool for detecting HIE.

CONFLICT OF INTEREST
None.

AUTHOR CONTRIBUTIONS
All authors contributed to the manuscript: LG wrote the manuscript and conceived and designed the work. JDJ and CG conceived and designed the work. RP, MS, LL, YH, DS and JDJ acquired, analyzed and interpreted the data. All authors substantively revised the manuscript.

REFERENCES
1. Kurinczuk JJ, White-Koning M, Badawi N. Epidemiology of neonatal encephalopathy and hypoxic-ischaemic encephalopathy. *Early Hum Dev.* 2010;86:329-338.

2. Chandraharan E Fetal scalp blood sampling during labour: is it a useful diagnostic test or a historical test that no longer has a place in modern clinical obstetrics? *BJOG* 2014;121:1056-1060; discussion 1060-1062.

3. Belfort MA, Saade GR, Thom E, et al. A randomized trial of intrapartum fetal ECG ST-segment analysis. *N Engl J Med*. 2015;373:632-641.

4. Graham EM, Adami RR, McKenney SL, Jennings JM, Burd I, Witter FR. Diagnostic accuracy of fetal heart rate monitoring in the identification of neonatal encephalopathy. *Obstet Gynecol*. 2014;124:507-513.

5. INFANT Collaborative Group. Computerised interpretation of fetal heart rate during labour (INFANT): a randomised controlled trial. *Lancet*. 2017;389:1719-1729.

6. Ruth VJ, Raivio KO. Perinatal brain damage: predictive value of metabolic acidosis and the Apgar score. *BMJ*. 1988;297:24-27.

7. Peeples ES, Rao R, Dizon MLV, et al. Predictive models of neurodevelopmental outcomes after neonatal hypoxic-ischemic encephalopathy. *Pediatrics*. 2021;147:e2020022962.

8. Tokuhisa T, Ibara S, Minakami H, Maede Y, Ishihara C, Matsui T. Outcome of infants with hypoxic ischemic encephalopathy treated with brain hypothermia. *J Obstet Gynaecol Res*. 2015;41:229-237.

9. van Ravenswaaij-Arts CM, Kollée LA, Hopman JC, Stoelinga GB, van Geijn HP. Heart rate variability. *Ann Intern Med*. 1993;118:436-447.

10. Canm J, Bigger T. Heart rate variability. Standards of measurement, physiological interpretation, and clinical use. Task Force of the European Society of Cardiology and the North American Society of Pacing and Electrophysiology. *Eur Heart J*. 1996;17:354-381.

11. Garabedian C, Champion C, Servan-Schreiber E, et al. A new analysis of heart rate variability in the assessment of fetal parasympathetic activity: an experimental study in a fetal sheep model. *PLoS ONE*. 2017;12:e0180653.

12. Frasch MG, Müller T, Hoyer D, Weiss C, Schubert H, Schwab M. Nonlinear properties of vagal and sympathetic modulations of heart rate variability in ovine fetus near term. *Am J Physiol-Regul Integr Comp Physiol*. 2009;296:R702-R707.

13. Ghesquière L, De Jonckheere J, Drumez E, et al. Parasympathetic nervous system response to acidosis: evaluation in an experimental fetal sheep model. *Acta Obstet Gynecol Scand*. 2019;98:433-439.

14. Ghesquière L, De Jonckheere J, Storme L, Garabedian C. Measurement of fetal parasympathetic activity during labor: a new pathway for evaluation of fetal well-being? *Am J Physiol Regul Integr Comp Physiol*. 2021;320:R467-R468.

15. Bersani I, Piersigilli F, Gazzolo D, et al. Heart rate variability as possible marker of brain damage in neonates with hypoxic ischemic encephalopathy: a systematic review. *Eur J Pediatr*. 2021;180:1335-1345.

16. Sarnat HB, Sarnat MS. Neonatal Encephalopathy Following Fetal Distress: A Clinical and Electroencephalographic Study. *Arch Neurol*. 1976;33:696-705.

17. Syutkina EV. Effect of autonomic nervous system blockade and acute asphyxia on heart rate variability in the fetal rat. *Gynecol Obstet Invest*. 1988;25:249-257.

18. Gold N, Frasch MG. Fetal cerebral perfusion is better than fetal acidaemia for the prediction of brain injury and might be assessable by sophisticated fetal heart rate metrics. *BJOG*. 2021;128:1443.

19. Garabedian C, Clermont-Hama Y, Sharma D, et al. Correlation of a new index reflecting the fluctuation of parasympathetic tone and fetal acidosis in an experimental study in a sheep model. *PLoS ONE*. 2018;13:e0190463.

20. Vanspranghels R, De Jonckheere J, Drumez E, et al. Autonomic response to fetal acidosis using an experimental sheep model. *Eur J Obstet Gynecol Reprod Biol*. 2020;246:151-155.

21. Prout AP, Frasch MG, Veldhuizen RAW, Hammond R, Ross MG, Richardson BS. Systemic and cerebral inflammatory response to umbilical cord occlusions with worsening acidosis in the ovine fetus. *Am J Obstet Gynecol*. 2010;202:82.e1-82.e9.

22. Logier R, Gehin AL, Bayart M, et al. Detection of transient myocardial ischemia by numerical processing of the electrocardiographic signal. *Proceeding of the IMACs conference*. 1994. p. 172–175.

23. Logier R, De Jonckheere J, Dassonneville A. An efficient algorithm for R-R intervals series filtering. *Conf Proc IEEE Eng Med Biol Soc*. 2004;2004:3937-3940.

24. Logier R, De Jonckheere J, Jeanne M, Matis R. Fetal distress diagnosis using heart rate variability analysis: design of a high frequency variability index. *Annu Int Conf IEEE Eng Med Biol Soc*. 2008;2008:4728-4731.

25. Mena H, Cadavid D, Rushing EJ. Human cerebral infarct: a proposed histopathologic classification based on 137 cases. *Acta Neuropathol*. 2004;108:524-530.

26. Garcia JH, Yoshida Y, Chen H, et al. Progression from ischemic injury to infarct following middle cerebral artery occlusion in the rat. *Am J Pathol*. 1993;142:623-635.

27. Garcia JH, Kamijyo Y. Cerebral infarction. Evolution of histopathological changes after occlusion of a middle cerebral artery in primates. *J Neuropathol Exp Neurol*. 1974;33:408-421.

28. Chuaqui R, Tapia J. Histologic assessment of the age of recent brain infarcts in man. *J Neuropathol Exp Neurol*. 1993;52:481-489.

29. Guilbaud L, Garabedian C, Di Rocco F, et al. Limits of the surgically induced model of myelomeningocele in the fetal sheep. *Childs Nerv Syst*. 2014;30:1425-1429.

30. Kilkenny C, Browne WJ, Cuthill IC, Emerson M, Altman DG. Improving Bioscience Research Reporting: The ARRIVE Guidelines for Reporting Animal Research. *PLoS Biol*. 2010;8:e1000412.

31. Kelly R, Ramaiah SM, Sheridan H, et al. Dose-dependent relationship between acidosis at birth and likelihood of death or cerebral palsy. *Arch Dis Child Fetal Neonatal Ed*. 2018;103:F567-F572.

32. Clark SL, Hamilton EF, Garite TJ, Timmins A, Warrick PA, Smith S. The limits of electronic fetal heart rate monitoring in the prevention of neonatal metabolic acidemia. *Am J Obstet Gynecol*. 2017;216:163.e1-163.e6.

33. Hafström M, Ehnberg S, Blad S, et al. Developmental outcome at 6.5 years after acidosis in term newborns: a population-based study. *Pediatrics*. 2012;129:e1501-e1507.

34. Georgieva A, Lear CA, Westgate JA, et al. Deceleration area and capacity during labour-like umbilical cord occlusions identify evolving hypotension: a controlled study in fetal sheep. *BJOG*. 2021;128:1433-1442.

35. Lear CA, Kasai M, Drury PP, et al. Plasma vasopressin levels are closely associated with fetal hypotension and neuronal injury after hypoxia-ischemia in near-term fetal sheep. *Pediatr Res*. 2020;88:857-864.

36. Gunn AJ, Maxwell L, De Haan HH, et al. Delayed hypotension and subendocardial injury after repeated umbilical cord occlusion in near-term fetal lambs. *Am J Obstet Gynecol*. 2000;183:1564-1572.

37. George S, Gunn AJ, Westgate JA, Brabyn C, Guan J, Bennet L. Fetal heart rate variability and brain stem injury after asphyxia in preterm fetal sheep. *Am J Physiol Regul Integr Comp Physiol*. 2004;287:R925-R933.

38. Turner JM, Mitchell MD, Kumar SS. The physiology of intrapartum fetal compromise at term. *Am J Obstet Gynecol*. 2020;222:17-26.

39. Evans MI, Eden RD, Britt DW, Evans SM, Schifrin BS. Re-engineering the interpretation of electronic fetal monitoring to identify reversible risk for cerebral palsy: a case control series. *J Matern Fetal Neonatal Med*. 2019;32:2561-2569.

40. Lear CA, Galinsky R, Wassink G, et al. The myths and physiology surrounding intrapartum decelerations: the critical role of the peripheral chemoreflex. *J Physiol*. 2016;594:4711-4725.

41. Yamaguchi K, Lear CA, Beacom MJ, Ikeda T, Gunn AJ, Bennet L. Evolving changes in fetal heart rate variability and brain

injury after hypoxia-ischaemia in preterm fetal sheep. *J Physiol.* 2018;596:6093-6104.

42. Lear CA, Galinsky R, Wassink G, et al. Sympathetic neural activation does not mediate heart rate variability during repeated brief umbilical cord occlusions in near-term fetal sheep. *J Physiol.* 2016;594:1265-1277.

43. Georgieva A, Abry P, Chudáček V, et al. Computer-based intrapartum fetal monitoring and beyond: A review of the 2nd Workshop on Signal Processing and Monitoring in Labor (October 2017, Oxford, UK). *Acta Obstet Gynecol Scand.* 2019;98:1207-1217.

44. Koehler RC, Yang Z-J, Lee JK, Martin LJ. Perinatal hypoxic-ischemic brain injury in large animal models: Relevance to human neonatal encephalopathy. *J Cereb Blood Flow Metab.* 2018;38:2092-2111.

45. Morrison JL, Berry MJ, Botting KJ, et al. Improving pregnancy outcomes in humans through studies in sheep. *Am J Physiol Regul Integr Comp Physiol.* 2018;315:R1123-R1153.

46. Bennet L, Westgate JA, Liu Y-CJ, Wassink G, Gunn AJ. Fetal acidosis and hypotension during repeated umbilical cord occlusions are associated with enhanced chemoreflex responses in near-term fetal sheep. *J Appl Physiol (Bethesda MD).* 1985;2005(99):1477-1482.

47. Frasch MG, Mansano RZ, Gagnon R, Richardson BS, Ross MG. Measures of acidosis with repetitive umbilical cord occlusions leading to fetal asphyxia in the near-term ovine fetus. *Am J Obstet Gynecol.* 2009;200:200.e1-200.e7.

48. Xu A, Matushewski B, Nygard K, Hammond R, Frasch MG, Richardson BS. Brain injury and inflammatory response to umbilical cord occlusions is limited with worsening acidosis in the near-term ovine fetus. *Reprod Sci.* 2016;23:858-870.

ORCID

Louise Ghesquière 🔟 https://orcid.org/0000-0003-4142-5526
Charles Garabedian 🔟 https://orcid.org/0000-0003-2105-9784

SUPPORTING INFORMATION

Additional supporting information may be found in the online version of the article at the publisher's website.